Directed Evolution of a Surface-Displayed Artificial Allylic Deallylase Relying on a GFP Reporter Protein

Alain Baiyoumy,[#] Jaicy Vallapurackal,[#] Fabian Schwizer,[#] Tillmann Heinisch, Tsvetan Kardashliev, Martin Held, Sven Panke, and Thomas R. Ward*

Read Online

ACCESS | Metrics & More | Article Recommendations | Supporting Information

ABSTRACT: Artificial metalloenzymes (ArMs) combine characteristics of both homogeneous catalysts and enzymes. Merging abiotic and biotic features allows for the implementation of new-to-nature reactions in living organisms. Here, we present the directed evolution of an artificial metalloenzyme based on *Escherichia coli* surface-displayed streptavidin (Sav^{SD} hereafter). Through the binding of a ruthenium-pianostool cofactor to Sav^{SD}, an artificial allylic deallylase (ADAse hereafter) is assembled, which displays catalytic activity toward the deprotection of alloc-protected 3-hydroxyaniline. The uncaged aminophenol acts as a gene switch and triggers the overexpression of a fluorescent green fluorescent protein (GFP) reporter protein. This straightforward readout of ADAse activity allowed the simultaneous saturation mutagenesis of two amino acid residues in Sav near the ruthenium cofactor, expediting the screening of 2762 individual clones. A 1.7-fold increase of *in vivo* activity was observed for Sav^{SD} S112T-K121G compared to the wild-type Sav^{SD} (wt-Sav^{SD}). Finally, the best performing Sav isoforms were purified and tested *in vitro* (Sav^{PP} hereafter). For Sav^{PP} S112M-K121A, a total turnover number of 372 was achieved, corresponding to a 5.9-fold increase vs wt-Sav^{PP}. To analyze the marked difference in activity observed between the surface-displayed and purified ArMs, the oligomeric state of Sav^{SD} was determined. For this purpose, crosslinking experiments of *E. coli* cells overexpressing Sav^{SD} were carried out, followed by sodium dodecyl sulfate−polyacrylamide gel electrophoresis (SDS-PAGE) and Western blot. The data suggest that Sav^{SD} is most likely displayed as a monomer on the surface of *E. coli*. We hypothesize that the difference between the *in vivo* and *in vitro* screening results may reflect the difference in the oligomeric state of Sav^{SD} vs soluble Sav^{PP} (monomeric vs tetrameric). Accordingly, care should be applied when evolving oligomeric proteins using *E. coli* surface display.
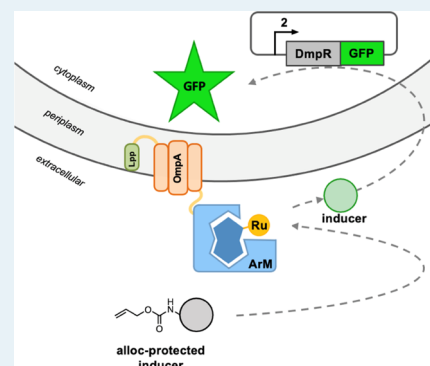
KEYWORDS: *directed evolution, in vivo screening, surface display, deallylation, purified protein screening*

INTRODUCTION

Artificial metalloenzymes[1] (ArMs) are formed by the incorporation of a synthetic cofactor into a natural host protein.[2,3] Artificial metalloenzymes combine the advantages of synthetic transition metal catalysts (e.g., broad range of reactivities,[4−13] large substrate scope, wide choice of metals) with the benefits of enzymes (e.g., high selectivity, high TON, aqueous compatibility, directed evolution).[8,9,11,13−18] Hence, such entities can be optimized by combining both chemical and genetic means, which significantly broadens the range of possible optimization approaches.[19] The effect of chemical or biological modifications can then be evaluated via a high-throughput screening[20] using various analytical readouts, including fluorescence or ultraperformance liquid chromatography-tandem mass spectrometry (UPLC-MS).[21,22]

Building on the pioneering work of Meggers,[23,24] we performed the *in vivo* deallylation of an alloc-protected aminocoumarin **5** moiety using an artificial allylic deallylase (hereafter ADAse).[25] The catalytic system, comprising an air and thiol tolerant ruthenium(II) complex **1**,[23] is anchored

within Sav^{SD} displayed on *Escherichia coli*'s outer membrane.[25,26] The efficiency of this system was improved via iterative saturation mutagenesis of the position S112 and K121.[17,27,28] The reaction was monitored via the fluorescence of the uncaged aminocoumarin **4**, Figure 1. We know from previous Sav-ArM evolution campaigns, that the iterative site-saturation mutagenesis at positions S112 and K121 often leads to significant improvement in catalytic performance, as these two positions lie in close proximity to the cofactor.[19,25,29] The possibility of expressing a protein at the surface of a cell[10,30−32] caught our attention since, relying on this process, we could avoid issues encountered using periplasmic or cytoplasmic expression (reductive conditions, limited accessibility of the
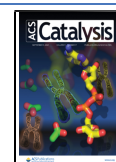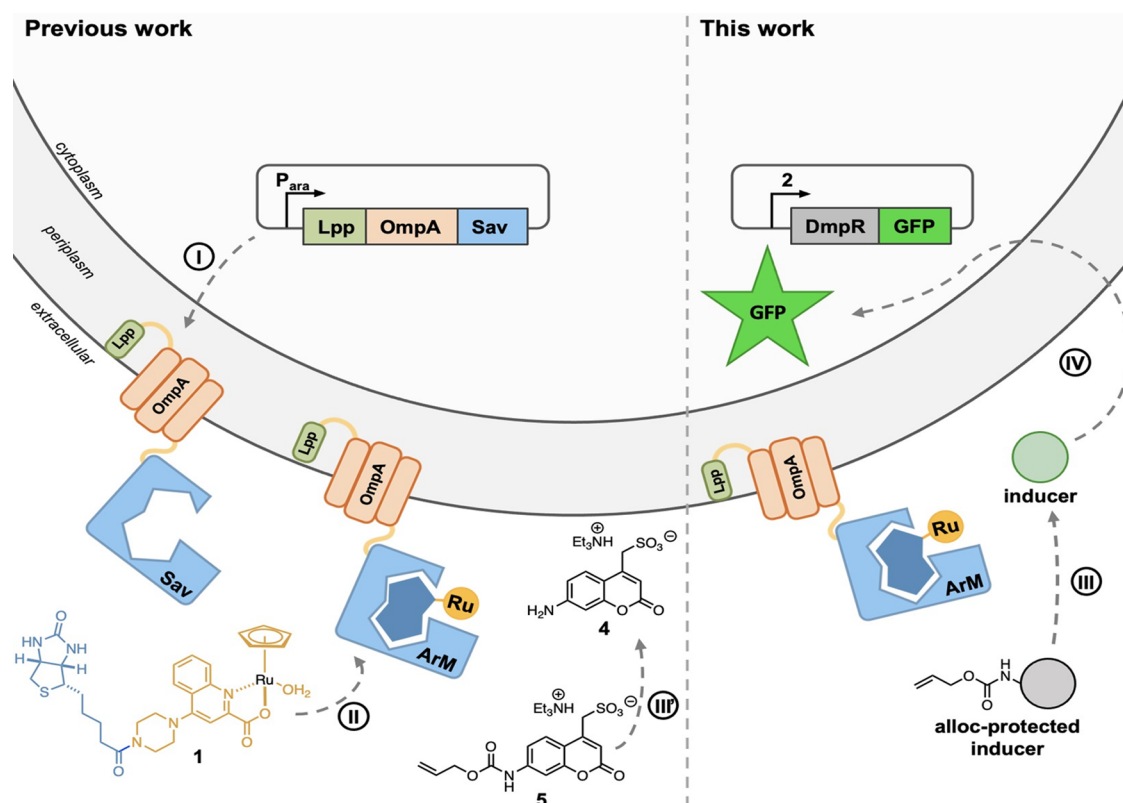
**Figure 1.** Comparison of previous and the current strategies for the optimization of ADAses using an *E. coli* surface-display construct. (I) Expression, translocation, and integration of the Lpp-OmpA-Sav construct on the outer membrane of *E. coli* cells. For clarity, only one streptavidin (Sav) monomer is displayed. (II) Biotinylated cofactor **1** binds to Sav^{SD} to afford the ADAse. Previous work: (III′) uncaging of the protected substrate **5** to yield the fluorescent coumarin **4**. This work: (III) uncaging of an alloc-protected inducer in the presence of the ADAse releases the inducer; (IV) the inducer diffuses into the cytoplasm of *E. coli* cells and induces the expression of GFP.
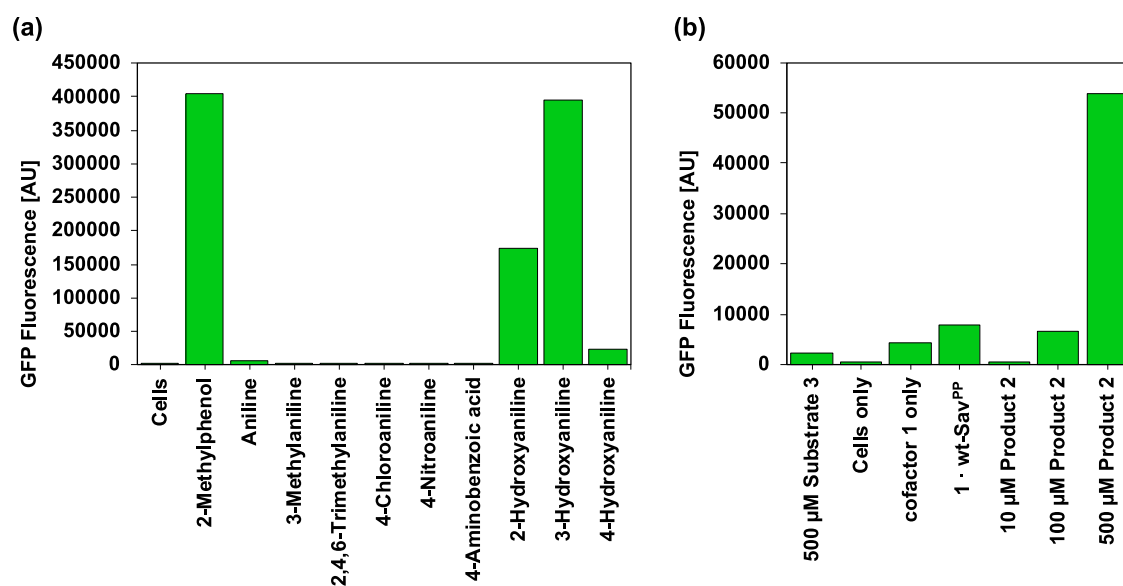

Figure 2. Identifying the best aromatic inducers and their response level toward GFP expression. (a) Induction capacity of various phenols and anilines for the DmpR regulator system. Reaction steps: (i) *E. coli* DH5α cells containing the DmpR-GFP reporter plasmid were cultivated in LB-medium at 30 °C to a cell density of $OD_{600} = 0.6$. (ii) Dilution of the cells to $OD_{600} = 0.05-0.08$, followed by the addition of 500 μM caged inducer. (iii) Incubation at 30 °C, 200 rpm shaking. (iv) Analysis of the fluorescence intensity of the cells by flow cytometry (the median value of the fluorescence intensity is displayed). (b) Performance of purified ADAses in the presence of reporter cells. Conditions: 500 μM substrate Alloc-protected 3-hydroxyaniline **3**, 5 μM ruthenium cofactor **1**, 2.5 μM wt-Sav^{PP}, 30 °C, and 9 h. Preparation of reporter cells (see the Supporting Information (SI)).

substrates, cofactors, etc.). Previous studies have highlighted the possibility of performing chemical transformations such as polymerization,[10] deallylation,[5,7,23,33] hydrolysis,[34] hydroarylation,[35] carbene insertion[8,36] in living cells environment and
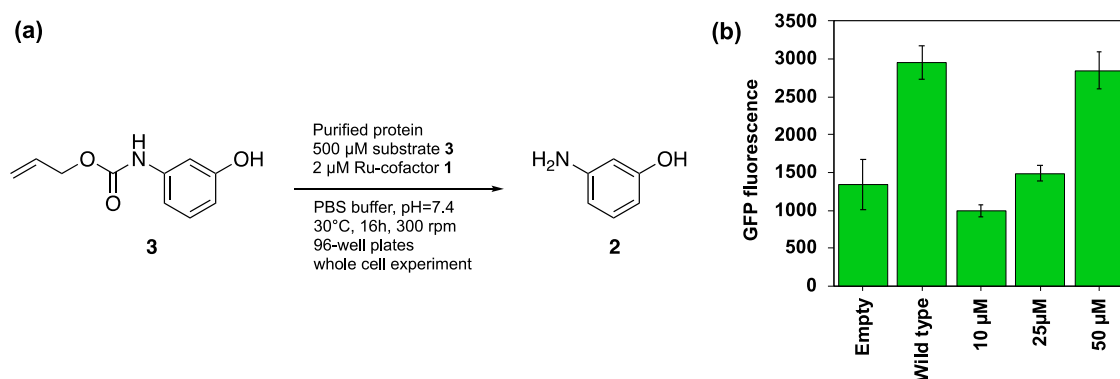
Figure 3. Uncaging Alloc-protected 3-hydroxyaniline **3** and resulting GFP fluorescence. (a) Reaction scheme and conditions for the allylic deallylation of the substrate **3** to the 3-hydroxyaniline **2**. Reaction conditions: 500 μM substrate **3**, incubation of cells with 2 μM cofactor **1**, 30 °C, 16 h. Preparation of catalysis cells using a normalized OD (see the SI). (b) Control experiments to validate the screening strategy: cells expressing wt-Sav^{SD} were spiked with 10, 25, or 50 μM product **2**. GFP fluorescence determined in a plate reader at: λ_{ex} = 475 nm; λ_{em} = 509 nm.
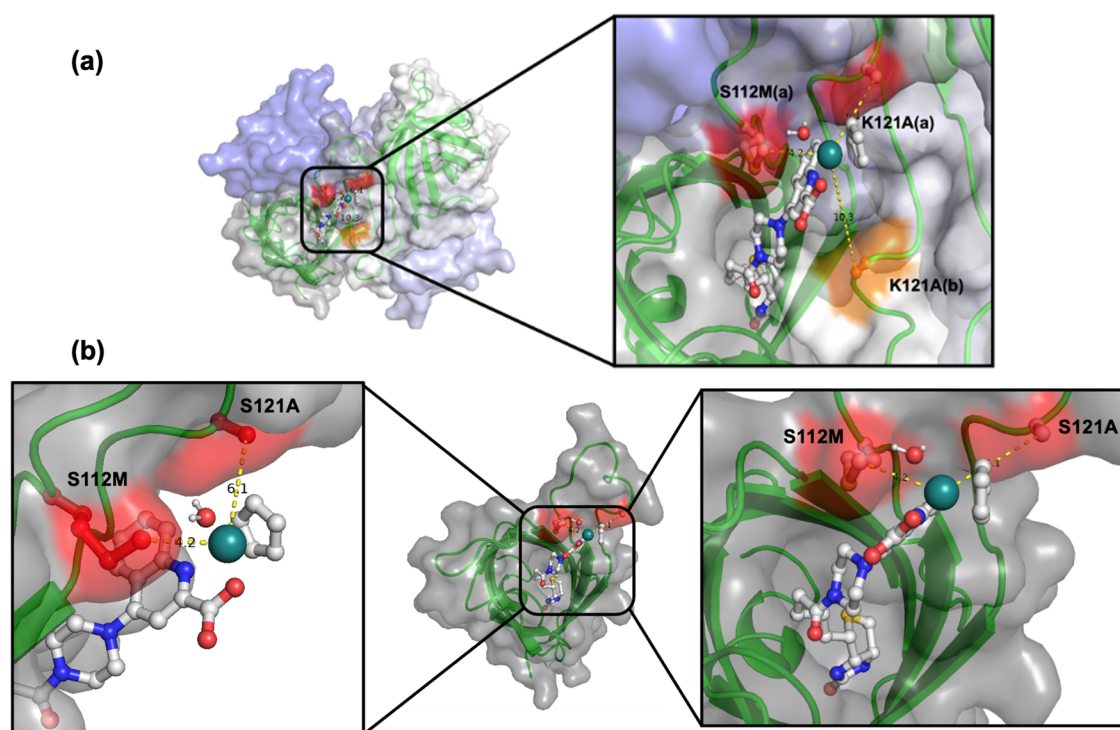

Figure 4. (a) Crystal structure of the ADAse $[CpRu(QA-Biot)(OH_2)]$ (**1**) · Sav S112M-K121A (PDB 6FH8[25]). The four monomeric units are displayed as transparent surface in gray, white, blue, and light blue. The mutated positions (S112M^a and K121A^a of monomer A) are highlighted in red and the position K121A^b of monomer B faces the active site is highlighted in orange (only in one of the two symmetry-related monomers). The biotinylated ruthenium complex is displayed as ball and stick. Color code: C = gray, N = blue, O = red, S = yellow, H = white, and Ru = dark green sphere. The cofactor **1** is anchored in the Sav monomer A (gray). The closest C_β-residue to Ru (dark green sphere) is K121A (red) of Sav monomer A (blue). (b) Computer-generated rendering of $[CpRu(QA-Biot)(OH_2)]$ (**1**) anchored in monomeric Sav S112M-K121A, highlighting the significant solvent exposure of the Ru-moiety and the resulting absence of contact between the cofactor and residue K121A of monomer b.

performing the uncaging of a fluorophore or an inducer in living cells.[7,25,37,38] More recently, we engineered a gene circuit in the cytoplasm of mammalian cells.[39] Based on these results, we aimed to develop a gene switch based on the regulatory protein DmpR[40−43] to promote the production of a protein of interest and allow us to monitor the improvement of the system via fluorescence. Building on these results, we set out to engineer and optimize an ArM whose activity could induce the overexpression of a reporter protein in *E. coli*. With this goal in mind, we selected the [CpRu]-catalyzed deallylation of amines, as pioneered by Meggers. We opted for an *E. coli* surface display of Sav to evolve the ADAse activity, relying on a

fluorescent readout caused by the upregulation of a green fluorescent protein reporter protein (GFP hereafter).

■ RESULTS AND DISCUSSION

To upregulate the GFP reporter protein in *E. coli*, we selected a DmpR-regulated GFP construct, whereby binding of various aniline/phenol derivatives to the DmpR regulator turns-on the overexpression of GFP, which can be conveniently used as readout of ADAse activity, Figure 1. As a first step, we tested the induction capacity of various polar benzene derivatives in the presence of reporter cells equipped with the DmpR-regulated GFP plasmid, Figure 2a. Both 2-methylphenol and 3-
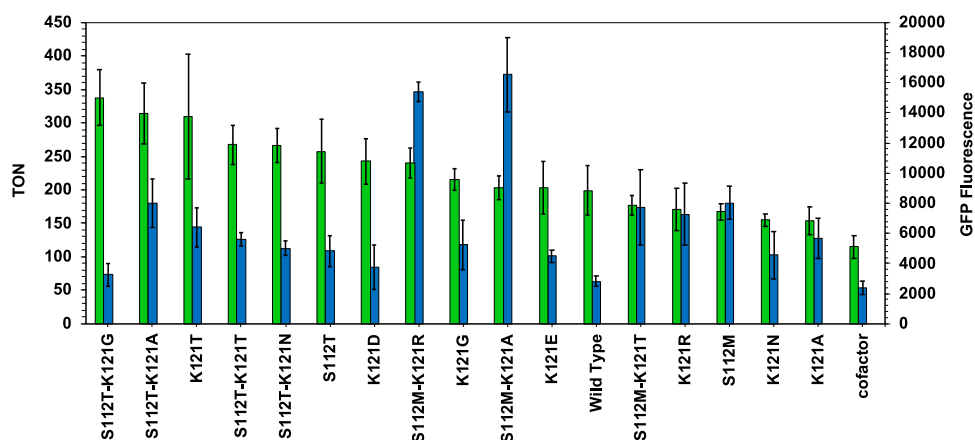
Figure 5. Directed evolution of artificial allylic deallylases for the uncaging of protected aniline **3**. *In vitro* catalysis (blue bars): Substrate **3** (500 μM), cofactor **1** (1 μM), purified Sav isoform (2 μM biotin-binding sites), phosphate-buffered saline (PBS) buffer (1×, pH 7.4), 30 °C, 18 h, and 300 rpm shaking. Total turnover number (TON) determined by high-performance liquid chromatography (HPLC; Figures S3 and S4). Error bars = standard deviation from triplicate measurements. *In vivo* catalysis (green bars): 500 μM substrate **3**, incubation of cells with 2 μM ruthenium cofactor **1**, 30 °C, and 16 h. Preparation of catalysis cells (see the SI). GFP fluorescence determined with a plate reader at: λ_{ex} = 475 nm; λ_{em} = 509 nm. Displayed values are normalized for the optical cell density (OD$_{600}$).

hydroxyaniline **2** performed best, as reflected by the GFP fluorescence observed in reporter cells. As allylcarbonates (to protect 2-methylphenol) are more prone to spontaneous hydrolysis than allylcarbamates (to protect 3-hydroxyaniline), we selected the *N*-allylcarbamate-3-hydroxyaniline **3** for further studies. Next, we spiked DmpR-GFP equipped reporter cells with the wild-type ADAse consisting of cofactor **1** · wt-Sav^{PP}, Figure 2b. We were pleased to observe the following trends: (i) the alloc-protected aniline **3** does not lead to marked GFP fluorescence in the reporter cells, (ii) the cofactor **1** alone is not very active at deprotecting compound **3**, and (iii) cofactor **1** · wt-Sav^{PP} leads to increased GFP fluorescence (1.8-fold vs cofactor **1** alone). The GFP fluorescence produced in the presence of cofactor **1** · wt-Sav^{PP} corresponds to the equivalent of spiking GFP-expressing cells with >100 μM 3-hydroxyaniline **2**. Based on these findings, we engineered a system based on two plasmids: Lpp-OmpA-Sav[26,44] and DmpR-GFP,[40,42,43] thus allowing us to screen and optimize the ADAse activity using a single cell. Lpp-OmpA-Sav regulates the expression and translocation of Sav to the surface of *E. coli* cells and is induced by L-arabinose, Figure 1. DmpR-GFP expresses a GFP reporter protein via the binding of an inducer to the DmpR regulator, Figure 1.

Next, we combined the previously designed *E. coli* surface-displayed ADAses with the deprotection of caged inducer **3** and the subsequent expression of GFP, Figure 3a. Control experiments revealed a modest background fluorescence for cells containing an empty vector (i.e., Lpp-OmpA plasmid without Sav gene), 2 μM cofactor **1**, and 500 μM caged substrate **3**, Figure 3b. Gratifyingly, in the presence of the assembled ADAse **1** · wt-Sav^{SD}, a 1.7-fold increased fluorescence was observed. The observed fluorescence is comparable to a GFP expression level in the presence of ∼50 μM 3-hydroxyaniline **2**. These highlight the reliability of the surface-displayed ADAse for screening purposes.

To validate the GFP-reporter strategy, we optimized the performance of the surface-displayed ADAse by simultaneously randomizing both S112 and K121 positions, Figure 4. Simultaneous saturation mutagenesis of two residues yields a library containing 20^2 = 400 different mutants in one pot. The screening effort (i.e., the oversampling) can be reduced by a

factor ∼1.8 (1724 colonies instead of 3066 colonies with a sequence coverage of 95%) when using the degenerate codon DNK instead of NNK.[19] This library comprises 17 different amino acids at each position (Gln, Pro, and His are missing), leading to a total number of 17^2 = 289 individual mutants.

The corresponding Sav^{SD} library was assembled by Gibson assembly including a synthesized part of the Sav gene that carried the required mutations at its center (90 base pair length, DNK codons in positions S112 and K121) into the Lpp-OmpA plasmid (see the SI). Analysis of the library revealed a good statistical distribution of the different amino acids, Figure S5. However, the library contained a background of 42% (i.e., original Lpp-OmpA plasmid, frame shifts, stop codons, inserts, unclear sequencing results). Thus, a coverage of 93.8% is predicted for a total of 2762 screened individual colonies.[45] The 2762 colonies were tested and the 88 most active clones were sequenced (see the SI for details). The 88 clones were retested to exclude false positives. Out of these 88 clones, the 10 best mutants (Sav^{SD} K121D, K121E, K121G, K121N, S112M-K121R, S112M-K121T, S112T-K121A, S112T-K121G, S112T-K121N, and S112T-K121T) were selected for protein expression in the cytoplasm, purification, and *in vitro* characterization.

Since almost all double mutants were more active than wt-Sav^{SD}, we also tested the corresponding single mutants (i.e., Sav^{PP} S112M, S112T, K121A, K121G, K121N, K121R, and K121T) to identify potential synergetic effects. In addition, streptavidin wild-type (wt-Sav^{PP}), Sav^{PP} mutant S112M-K121A (i.e., the best mutant identified in previous work[25]), as well as the cofactor **1** alone, were included in the *in vitro* catalysis validation (Figure 5). Comparison of the *in vivo* and *in vitro* ADAse activities revealed striking differences, Figure 5. Although variable expression levels may account for marked differences *in vivo* enzymatic activities (Figure S6),[25] past experience with Sav expression levels[28] led us to investigate an alternative hypothesis. Indeed, we surmised that fusing each Sav monomer (16.7 kDa) with a hydrophobic Lpp-OmpA insert (15.3 kDa) may affect the quaternary structure of surface-displayed Sav. Since two monomers of Sav make up the biotin-binding vestibule (Figure 4), the oligomeric nature of Sav may strongly affect which close-lying mutation of surface-

displayed Sav (quaternary structure unknown) is indeed present in purified, tetrameric Sav[PP] samples.[26,46,47]

To assess the quaternary structure of surface-displayed Lpp-OmpA-Sav, we set out to: (i) treat *E. coli* cells with a crosslinking agent, (ii) lyse the cells, and (iii) analyze the protein content by sodium dodecyl sulfate—polyacrylamide gel electrophoresis (SDS-PAGE) and Western blot to identify the Sav-containing bands. Although surface display is a widely used strategy in protein expression and optimization, the quaternary structure of oligomeric, surface-displayed, proteins should to be addressed on a case-to-case basis.[44,48,49]

To minimize the adventitious assembly of homotetrameric Sav following cell lysis and workup, the cells were treated with bis(sulfosuccinimidyl) suberate (BS[3]), a protein crosslinking agent,[50] to fix the oligomeric state of Sav[SD] prior to cell lysis (Figure 6). Similar studies have highlighted the crosslinking of *E. coli* outer membrane proteins using cleavable crosslinkers to yield oligomeric proteins.[51−53] Exploratory crosslinking experiments highlighted the superiority of the anionic BS[3] vs the commonly used glutaraldehyde.[50,51] The Sav[SD]—as well as the empty vector as negative control—were expressed in *E. coli* at 25 °C for 24 h in shaking flasks. The cells were harvested and the pellets were washed with PBS and resuspended in PBS before crosslinking with BS[3] (8 mM, 30 min, 25 °C) (see the SI for details). The crosslinking was quenched by addition of 1 M tris-buffer, the cell suspension centrifuged, the supernatant discarded, and the cell pellet was resuspended in lysis buffer, which is supposed to release the Sav from the cellular environment and render it in the supernatant. The suspension was centrifuged and the supernatant was set aside for analysis. One part of the supernatant was loaded onto the gel (Figure 7, lane 6/9) and one part was denatured (SDS sample buffer, 95 °C, 30 min), Figure 7, lane 7/10. The remaining cell pellet was resuspended in 8 M urea to ensure the recovery of any additional protein that might have been retained in the cell debris from lysis, centrifuged, and the supernatant was subjected to analysis, Figure 7, lane 8/11. For comparison, wt-Sav[PP] was subjected to crosslinking with BS[3]. The resulting protein samples were analyzed by SDS-PAGE, Figure 7. To validate the BS[3] crosslinking strategy, control experiments using wt-Sav[PP] were carried out. From this treatment, the following observations can be made: (i) The Sav[PP] samples that were first denatured and then crosslinked mainly appear as monomers and partly as dimers, Figure 7, lane 5. (ii) In contrast, the denatured Sav[PP] sample that was not crosslinked mainly migrates as monomer, dimer, as well as tetramer and higher oligomers on the SDS-PAGE, Figure 7, lane 2. This highlights the exceptional stability of Sav in the presence of chaotropic agents. (iii) The Sav[PP] samples that were crosslinked before the denaturation step retain their tetrameric structure, Figure 7, lane 4. We thus conclude that BS[3] crosslinking strategy permanently fixes the oligomeric state of Sav. Importantly, the fixed oligomeric state is not affected by subsequent denaturation.

Next, we analyzed the surface-displayed constructs, following the above strategy. For Sav[SD], the electrophoresis results performed on a crosslinked Sav[SD] sample strongly suggest that Sav[SD] is displayed mostly as a monomer on the *E. coli*'s surface. Form the data displayed in Figure 7, the following observations can be made: (i) the samples denatured prior to crosslinking display a prominent band at about 32 kDa (Figure 7, lanes 10 and 11). This band corresponds to the molecular weight of monomeric Sav[SD] (Lpp-OmpA-Sav 31.925 kDa). (ii) The
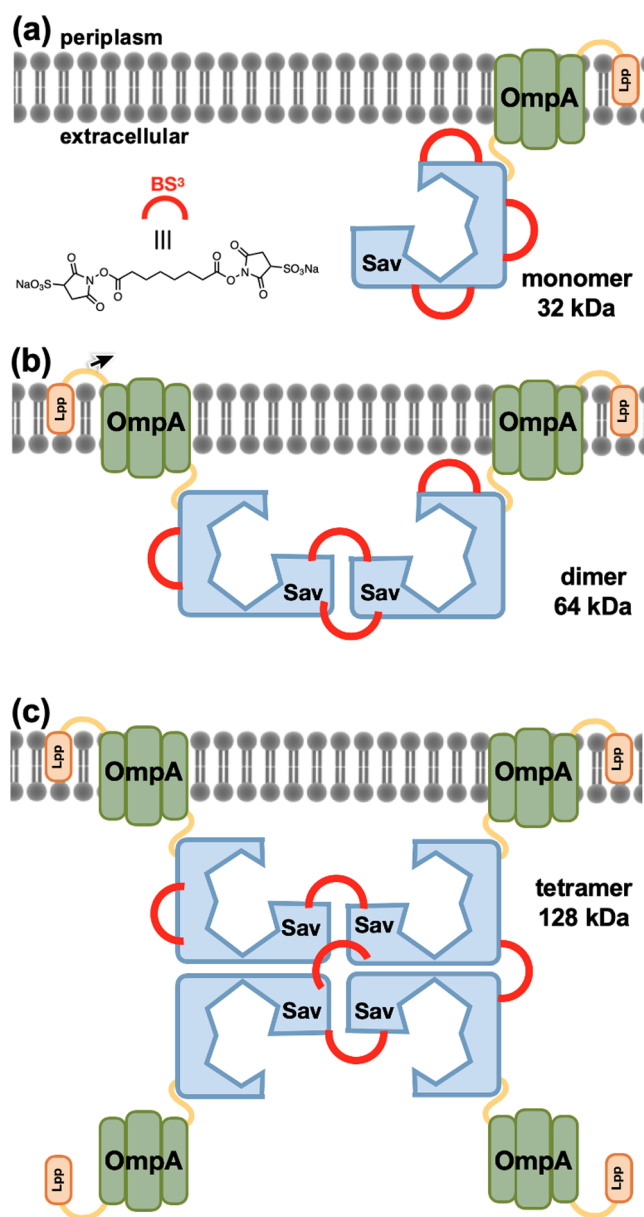

Figure 6. Schematic representation of Sav[SD] using the Lpp-OmpA display system and the crosslinking approach. (a) Crosslinking with bis(sulfosuccinimidyl) suberate (BS[3]), which mainly targets lysines, fixes the oligomeric state of the surface-displayed Sav[SD]. Subsequent lysis of the cell membrane releases the crosslinked constructs into the solution that are analyzed by SDS-PAGE and western blot (see Figure 7). Depending on the surface-displayed quaternary structure of Sav[SD], three different sizes—(a) 32 kDa, (b) 64 kDa, and (c) 128 kDa—can be expected for the monomer, dimer, and tetramer, respectively.

nondenatured Sav[SD] sample (Figure 7, lane 9) displays faint bands at higher molecular weights. These bands arise as a result of the remarkable stability of homotetrameric Sav. Indeed, despite the chaotropic nature of SDS-page, non-crosslinked Sav tends to oligomerize (tetramer and higher oligomers) under these conditions. This behavior was also observed for Sav[PP], Figure 7, lanes 1−5.[54]

Based on these qualitative observations, we hypothesize that the Lpp-OmpA-Sav is not displayed as a homotetramer on the outer membrane of *E. coli*.

Inspection of the X-ray crystal structure of [CpRu(QA−Biot)(OH₂)] (**1**) · Sav S112M-K121A (PDB 6FH8[25])
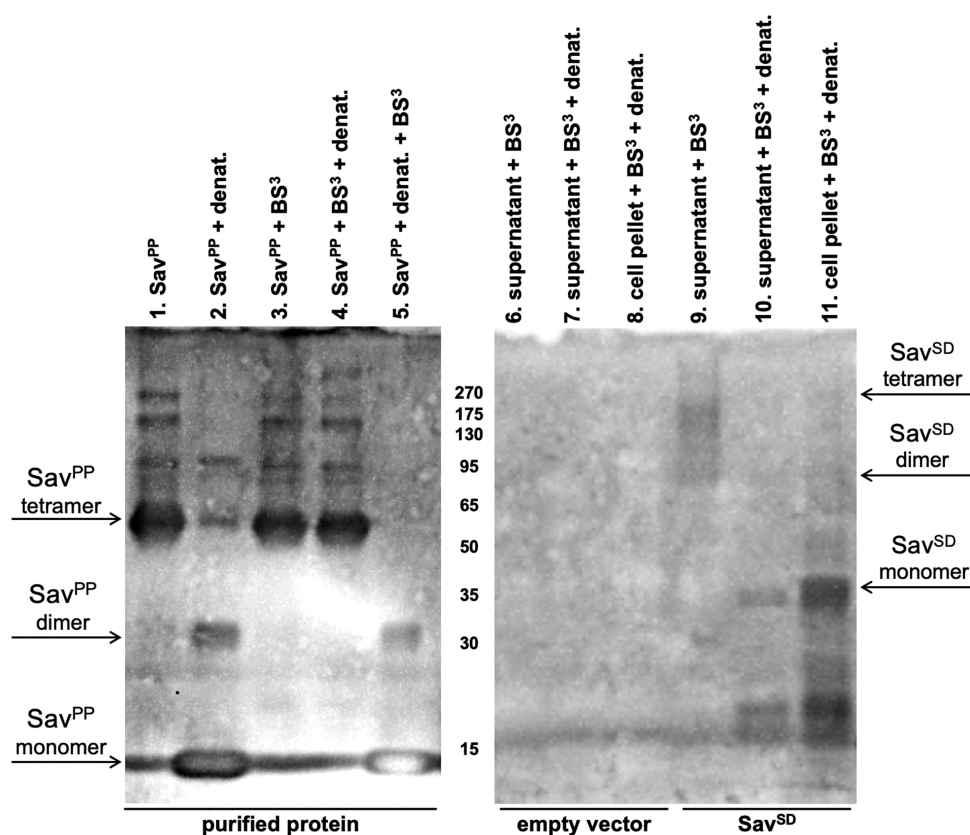
Figure 7. Western blot analysis of the quaternary structure of Sav^{SD}. Crosslinking of Sav^{SD}, followed by SDS-PAGE (14% polyacrylamide gel) and western blot (anti-Sav rabbit polyclonal antibody used at a 1:200 dilution). Lanes 1 and 2 were not crosslinked. For lanes 3−11, except for lane 5, all samples were crosslinked with BS^3 prior to any additional treatment. All denatured samples were treated under the same conditions: SDS sample buffer, 95 °C, and 30 min. (1) Sav^{PP}, (2) denatured Sav^{PP}, (3) crosslinked Sav^{PP}, (4) crosslinked and then denatured Sav^{PP}, (5) denatured and then crosslinked Sav^{PP}, (6) empty vector, supernatant, (7) empty vector, denatured supernatant, (8) empty vector, denatured cell pellet (9) Sav^{SD}, supernatant, (10) Sav^{SD}, denatured supernatant, and (11) Sav^{SD}, denatured cell pellet.

highlights the position of the Ru-moiety at the interface between two Sav monomers, Figure 4a. By (virtually) removing the adjacent monomer Sav (b), the cofactor becomes significantly less shielded by Sav. Importantly, the close contact with the residue at position 121 (b) is no longer present, Figure 4b. As a consequence, the randomization of residue K121X affects the performance of the deallylase differently in monomeric Sav—as only K121X of monomer (a) affects catalytic performance—vs tetrameric Sav—whereby both K121X (a) and K121X (b) lie in the proximity of the Ru cofactor, Figure 4. As it is challenging to predict which of the two K121X residues affect catalytic performance most, the *in vitro* validation with homotetrameric Sav differs on a case to case when compared to the surface-display screen, whereby Sav is displayed (mostly) as a monomeric protein.

In summary, care are should be applied when optimizing the performance of surface-displayed oligomeric (artificial) enzymes, especially if their active site lies at the interface between monomers, as is the case for streptavidin, Figure 4.

CONCLUSIONS

An *E. coli* surface-displayed artificial allylic deallylase has been engineered to turn on a gene switch leading to the upregulation of GFP. The ADAse activity was genetically optimized by simultaneous site-saturation mutagenesis of positions S112 and K121. The most active surface-displayed ADAase (Sav^{SD}- S112T-K121G) revealed a 1.7-fold improve-

ment compared to the wild-type Sav ADAse. However, validation of surface-displayed ADAse with purified Sav samples revealed marked differences between Sav^{SD} and Sav^{PP} data. Using Sav^{PP}, the best variant was Sav^{PP} S112M-K121A with a 5.9-fold increase (and TON = 372) in catalytic activity compared to the ADAse based on wild type. The differences in activity between surface-displayed ArMs and purified samples—reflected by GFP fluorescence and 3-hydroxyaniline **2** detected by HPLC—may be the result of multiple parameters: (i) Sav^{SD} expression levels, the presence of side products, including the formation of *N*-allylated 3-hydroxyaniline[6] and (ii) oligomeric nature of Sav^{SD}. Experimental evidence presented herein strongly supports the latter hypothesis. In conclusion, we favor the periplasmic screening of oligomeric ArMs over the surface display strategy as the periplamsic screen leads to more comparable results to those obtained with purified proteins.[28]

■ ASSOCIATED CONTENT

ⓢ Supporting Information

The Supporting Information is available free of charge at https://pubs.acs.org/doi/10.1021/acscatal.1c02405.

> Design and expression of streptavidin mutants, experimental procedure;
>
> instruments and materials; expression and purification of streptavidin isoforms; synthesis of the biotinylated ruthenium cofactor brief description; design of a caged

DmpR substrate; *in vitro* catalysis; design, cloning, and transformation of streptavidin and reporter plasmids; and catalysis with GFP reporter cells (PDF)

■ AUTHOR INFORMATION

Corresponding Author

Thomas R. Ward − *Department of Chemistry, University of Basel, 4058 Basel, Switzerland; Molecular Systems Engineering, National Competence Center in Research (NCCR), 4058 Basel, Switzerland;* ● orcid.org/0000-0001-8602-5468; Email: thomas.ward@unibas.ch

Authors

Alain Baiyoumy − *Department of Chemistry, University of Basel, 4058 Basel, Switzerland; Molecular Systems Engineering, National Competence Center in Research (NCCR), 4058 Basel, Switzerland;* ● orcid.org/0000-0003-3007-4724

Jaicy Vallapurackal − *Department of Chemistry, University of Basel, 4058 Basel, Switzerland; Molecular Systems Engineering, National Competence Center in Research (NCCR), 4058 Basel, Switzerland*

Fabian Schwizer − *Department of Chemistry, University of Basel, 4058 Basel, Switzerland; Present Address: Interlabor Belp AG, Aemmenmattstrasse 16, CH-3123 Belp, Switzerland*

Tillmann Heinisch − *Department of Chemistry, University of Basel, 4058 Basel, Switzerland; Present Address: DNA Script, 67 avenue de Fontainebleau, 94270, Le Kremlin-Bicêtre, France*

Tsvetan Kardashliev − *ETH Zürich, D-BSSE, 4058 Basel, Switzerland*

Martin Held − *ETH Zürich, D-BSSE, 4058 Basel, Switzerland*

Sven Panke − *ETH Zürich, D-BSSE, 4058 Basel, Switzerland; Molecular Systems Engineering, National Competence Center in Research (NCCR), 4058 Basel, Switzerland*

Complete contact information is available at:
https://pubs.acs.org/10.1021/acscatal.1c02405

Author Contributions

[#]A.B., J.V., and F.S. contributed equally to this work.

Author Contributions

General concepts and idea by T.R.W. Cloning of the constructs and library creation by T.H., T.K., and F.S. A.B. and F.S. performed the *in vivo* and *in vitro* experiments. A.B. performed the *in vitro* experiments and molecule characterizations via HPLC. J.V. designed and performed the cross-linking experiments. T.R.W., A.B. and J.V. wrote the manuscript. All authors reviewed the manuscript and the SI.

Notes

The authors declare no competing financial interest.

■ ABBREVIATIONS

Sav, streptavidin; ADAse, allylic deallylase; WT-ADAse · **1**, wild-type Sav with incorporated cofactor **1**; Sav[SD], surface-displayed streptavidin; BS[3], bis(sulfosuccinimidyl) suberate

■ REFERENCES

(1) Wilson, M. E.; Whitesides, G. M. Conversion of a Protein to a Homogeneous Asymmetric Hydrogenation Catalyst by Site-Specific Modification with a Diphosphinerhodium(I) Moiety. *J. Am. Chem. Soc.* **1978**, *100*, 306−307.

(2) Schwizer, F.; Okamoto, Y.; Heinisch, T.; Gu, Y.; Pellizzoni, M. M.; Lebrun, V.; Reuter, R.; Köhler, V.; Lewis, J. C.; Ward, T. R. Artificial Metalloenzymes: Reaction Scope and Optimization Strategies. *Chem. Rev.* **2018**, *118*, 142−231.

(3) Davis, H. J.; Ward, T. R. Artificial Metalloenzymes: Challenges and Opportunities. *ACS Cent. Sci.* **2019**, *5*, 1120−1136.

(4) Reetz, M. T.; Peyralans, J. J. P.; Maichele, A.; Fu, Y.; Maywald, M. Directed Evolution of Hybrid Enzymes: Evolving Enantioselectivity of an Achiral Rh-Complex Anchored to a Protein. *Chem. Commun.* **2006**, *113*, 4318−4320.

(5) Tomás-Gamasa, M.; Martínez-Calvo, M.; Couceiro, J. R.; Mascareñas, J. L. Transition Metal Catalysis in the Mitochondria of Living Cells. *Nat. Commun.* **2016**, No. 12538.

(6) Hsu, H. T.; Trantow, B. M.; Waymouth, R. M.; Wender, P. A. Bioorthogonal Catalysis: A General Method to Evaluate Metal-Catalyzed Reactions in Real Time in Living Systems Using a Cellular Luciferase Reporter System. *Bioconjugate Chem.* **2016**, *27*, 376−382.

(7) Völker, T.; Meggers, E. Chemical Activation in Blood Serum and Human Cell Culture: Improved Ruthenium Complex for Catalytic Uncaging of Alloc-Protected Amines. *ChemBioChem* **2017**, *18*, 1083−1086.

(8) Key, H. M.; Dydio, P.; Clark, D. S.; Hartwig, J. F. Abiological Catalysis by Artificial Haem Proteins Containing Noble Metals in Place of Iron. *Nature* **2016**, *534*, 534−537.

(9) Song, W. J.; Tezcan, F. A. A Designed Supramolecular Protein Assembly with in Vivo Enzymatic Activity. *Science* **2021**, *346*, 1525−1528.

(10) Grimm, A. R.; Sauer, D. F.; Polen, T.; Zhu, L.; Hayashi, T.; Okuda, J.; Schwaneberg, U. A Whole Cell E. coli Display Platform for Artificial Metalloenzymes: Poly(Phenylacetylene) Production with a Rhodium-Nitrobindin Metalloprotein. *ACS Catal.* **2018**, *8*, 2611−2614.

(11) Blomberg, R.; Kries, H.; Pinkas, D. M.; Mittl, P. R. E.; Grütter, M. G.; Privett, H. K.; Mayo, S. L.; Hilvert, D. Precision Is Essential for Efficient Catalysis in an Evolved Kemp Eliminase. *Nature* **2013**, *503*, 418−421.

(12) Srivastava, P.; Yang, H.; Ellis-Guardiola, K.; Lewis, J. C. Engineering a Dirhodium Artificial Metalloenzyme for Selective Olefin Cyclopropanation. *Nat. Commun.* **2015**, *6*, No. 7789.

(13) Destito, P.; Vidal, C.; López, F.; Mascareñas, J. L. Transition Metal-Promoted Reactions in Aqueous Media and Biological Settings. *Chem. - Eur. J.* **2021**, *27*, 4789−4816.

(14) Ilie, A.; Reetz, M. T. Directed Evolution of Artificial Metalloenzymes. *Isr. J. Chem.* **2015**, *55*, 51−60.

(15) Bornscheuer, U. T.; Huisman, G. W.; Kazlauskas, R. J.; Lutz, S.; Moore, J. C.; Robins, K. Engineering the Third Wave of Biocatalysis. *Nature* **2012**, *485*, 185−194.

(16) Brandenberg, O. F.; Fasan, R.; Arnold, F. H. Exploiting and Engineering Hemoproteins for Abiological Carbene and Nitrene Transfer Reactions. *Curr. Opin. Biotechnol.* **2017**, *47*, 102−111.

(17) Kille, S.; Acevedo-Rocha, C. G.; Parra, L. P.; Zhang, Z. G.; Opperman, D. J.; Reetz, M. T.; Acevedo, J. P. Reducing Codon Redundancy and Screening Effort of Combinatorial Protein Libraries Created by Saturation Mutagenesis. *ACS Synth. Biol.* **2013**, *2*, 83−92.

(18) Ward, T. R. Artificial Metalloenzymes Based on the Biotin - Avidin Technology: Enantioselective Catalysis and Beyond. *Acc. Chem. Res.* **2011**, *44*, 47−57.

(19) Jeschek, M.; Reuter, R.; Heinisch, T.; Trindler, C.; Klehr, J.; Panke, S.; Ward, T. R. Directed Evolution of Artificial Metalloenzymes for in Vivo Metathesis. *Nature* **2016**, *537*, 661−665.

(20) Nguyen, D. P.; Nguyen, H. T. H.; Do, L. H. Tools and Methods for Investigating Synthetic Metal-Catalyzed Reactions in Living Cells. *ACS Catal.* **2021**, *11*, 5148−5165.

(21) Markel, U.; Sauer, D. F.; Schiffels, J.; Okuda, J.; Schwaneberg, U. Towards the Evolution of Artificial Metalloenzymes—A Protein Engineer's Perspective. *Angew. Chem.* **2019**, *131*, 4500−4511.

(22) Obexer, R.; Godina, A.; Garrabou, X.; Mittl, P. R. E.; Baker, D.; Griffiths, A. D.; Hilvert, D. Emergence of a Catalytic Tetrad during Evolution of a Highly Active Artificial Aldolase. *Nat. Chem.* **2017**, *9*, 50−56.

(23) Völker, T.; Dempwolff, F.; Graumann, P. L.; Meggers, E. Progress towards Bioorthogonal Catalysis with Organometallic Compounds. *Angew. Chem., Int. Ed.*. **2014**, *53*, 10536−10540.

(24) Streu, C.; Meggers, E. Ruthenium-Induced Allylcarbamate Cleavage in Living Cells. *Angew. Chem., Int. Ed.* **2006**, *45*, 5645−5648.

(25) Heinisch, T.; Schwizer, F.; Garabedian, B.; Csibra, E.; Jeschek, M.; Vallapurackal, J.; Pinheiro, V. B.; Marlière, P.; Panke, S.; Ward, T. R. E. Coli Surface Display of Streptavidin for Directed Evolution of an Allylic Deallylase. *Chem. Sci.* **2018**, *9*, 5383−5388.

(26) Park, M.; Jose, J.; Thömmes, S.; Kim, J. I.; Kang, M. J.; Pyun, J. C. Autodisplay of Streptavidin. *Enzyme Microb. Technol.* **2011**, *48*, 307−311.

(27) Reetz, M. T.; Carballeira, J. D. Iterative Saturation Mutagenesis (ISM) for Rapid Directed Evolution of Functional Enzymes. *Nat. Protoc.* **2007**, *2*, 891−903.

(28) Vornholt, T.; Christoffel, F.; Pellizzoni, M. M.; Panke, S.; Ward, T. R.; Jeschek, M. Systematic Engineering of Artificial Metalloenzymes for New-to-Nature Reactions. *Sci. Adv.* **2021**, *7*, 4208−4230.

(29) Hestericová, M.; Heinisch, T.; Alonso-Cotchico, L.; Maréchal, J.-D.; Vidossich, P.; Ward, T. R. Directed Evolution of an Artificial Imine Reductase. *Angew. Chem.* **2018**, *130*, 1881−1886.

(30) Jose, J.; Bernhardt, R.; Hannemann, F. Functional Display of Active Bovine Adrenodoxin on the Surface of E. coli by Chemical Incorporation of the [2Fe ± 2S] Cluster. *ChemBioChem* **2001**, *2*, 695−701.

(31) Jose, J.; Von Schwichow, S. Autodisplay of Active Sorbitol Dehydrogenase (SDH) Yields a Whole Cell Biocatalyst for the Synthesis of Rare Sugars. *ChemBioChem* **2004**, *5*, 491−499.

(32) Peschke, T.; Rabe, K. S.; Niemeyer, C. M. Orthogonal Surface Tags for Whole-Cell Biocatalysis. *Angew. Chem. Int. Ed.* **2017**, *56*, 2183−2186.

(33) Hsu, H. T.; Trantow, B. M.; Waymouth, R. M.; Wender, P. A. Bioorthogonal Catalysis: A General Method to Evaluate Metal-Catalyzed Reactions in Real Time in Living Systems Using a Cellular Luciferase Reporter System. *Bioconjugate Chem.* **2016**, *27*, 376−382.

(34) Song, W. J.; Tezcan, F. A. A Designed Supramolecular Protein Assembly with in Vivo Enzymatic Activity. *Science* **2021**, *346*, 1525−1528.

(35) Vidal, C.; Tomás-Gamasa, M.; Destito, P.; López, F.; Mascareñas, J. L. Concurrent and Orthogonal Gold(I) and Ruthenium(II) Catalysis inside Living Cells. *Nat. Commun.* **2018**, *9*, No. 1913.

(36) Dydio, P.; Key, H. M.; Nazarenko, A.; Rha, J. Y.-E.; Seyedkazemi, V.; Clark, D. S.; Hartwig, J. F. An Artificial Metalloenzyme with the Kinetics of Native Enzymes. *Science* **2016**, *354*, 102−106.

(37) Rubini, R.; Mayer, C. Addicting Escherichia Coli to New-to-Nature Reactions. *ACS Chem. Biol.* **2020**, *15*, 3093−3098.

(38) Martínez-Calvo, M.; Mascareñas, J. L. Organometallic Catalysis in Biological Media and Living Settings. *Coord. Chem. Rev.* **2018**, *359*, 57−79.

(39) Okamoto, Y.; Kojima, R.; Schwizer, F.; Bartolami, E.; Heinisch, T.; Matile, S.; Fussenegger, M.; Ward, T. R. A Cell-Penetrating Artificial Metalloenzyme Regulates a Gene Switch in a Designer Mammalian Cell. *Nat. Commun.* **2018**, *9*, No. 1943.

(40) Shingler, V.; Moore, T. Sensing of Aromatic Compounds by the DmpR Transcriptional Activator of Phenol-Catabolizing Pseudomonas Sp. Strain CF600. *J. Bacteriol.* **1994**, *176*, 1555−1560.

(41) Shingler, V.; Bartilson, M.; Moore, T. Cloning and Nucleotide Sequence of the Gene Encoding the Positive Regulator (DmpR) of the Phenol Catabolic Pathway Encoded by PVI150 and Identification of DmpR as a Member of the NtrC Family of Transcriptional Activators. *J. Bacteriol.* **1993**, *175*, 1596−1604.

(42) Choi, S. L.; Rha, E.; Lee, S. J.; Kim, H.; Kwon, K.; Jeong, Y. S.; Rhee, Y. H.; Song, J. J.; Kim, H. S.; Lee, S. G. Toward a Generalized and High-Throughput Enzyme Screening System Based on Artificial Genetic Circuits. *ACS Synth. Biol.* **2014**, *3*, 163−171.

(43) Kwon, K. K.; Lee, D. H.; Kim, S. J.; Choi, S. L.; Rha, E.; Yeom, S. J.; Subhadra, B.; Lee, J.; Jeong, K. J.; Lee, S. G. Evolution of Enzymes with New Specificity by High-Throughput Screening Using DmpR-Based Genetic Circuits and Multiple Flow Cytometry Rounds. *Sci. Rep.* **2018**, *8*, No. 2659.

(44) Earhart, C. F. Use of an Lpp-OmpA Fusion Vehicle for Bacterial Surface Display. *Methods Enzym.* **2000**, *326*, 506−516.

(45) Reetz, M. T.; Sanchis, J. Constructing and Analyzing the Fitness Landscape of an Experimental Evolutionary Process. *ChemBioChem* **2008**, *9*, 2260−2267.

(46) Francisco, J. A.; Earhart, C. F.; Georgiou, G. Transport and Anchoring of ß-Lactamase to the External Surface of *Escherichia coli*. *Biochemistry* **1992**, *89*, 2713−2717.

(47) Jose, J.; Meyer, T. F. The Autodisplay Story, from Discovery to Biotechnical and Biomedical Applications. *Microbiol. Mol. Biol. Rev.* **2007**, *71*, 600−619.

(48) Stathopoulos, C.; Georgiou, G.; Earhart, C. F. Characterization of Escherichia Coli Expressing an Lpp′OmpA(46-159)-PhoA Fusion Protein Localized in the Outer Membrane. *Appl. Microbiol. Biotechnol.* **1996**, *45*, 112−119.

(49) van Bloois, E.; Winter, R. T.; Kolmar, H.; Fraaije, M. W. Decorating Microbes: Surface Display of Proteins on Escherichia Coli. *Trends Biotechnol.* **2011**, *29*, 79−86.

(50) Shi, J. M.; Pei, J.; Liu, E. Q.; Zhang, L. Bis(Sulfosuccinimidyl) Suberate (BS3) Crosslinking Analysis of the Behavior of Amyloid-ß Peptide in Solution and in Phospholipid Membranes. *PLoS One* **2017**, *12*, 1−13.

(51) Reinhart, A. F. R.; Bragg, P. D. Cross-Linking of the Proteins in the Outer Membrane of Escherichia Coli. *Biochim. Biophys. Acta, Biomembr.* **1977**, *466*, 245−256.

(52) Palva, E. T.; Rndall, L. L. Nearest-Neighbor Analysis of *Escherichia coli* Outer Membrane Proteins, Using Cleavable Cross-Links. *J. Bacteriol.* **1976**, *127*, 1558−1560.

(53) Angus, B. L.; Hancock, R. E. W. Outer Membrane Porin Proteins F, P, and D1 of Pseudomonas Aeruginosa and PhoE of Escherichia Coli: Chemical Cross-Linking to Reveal Native Oligomers. *J. Bacteriol.* **1983**, *155*, 1042−1051.

(54) Humbert, N.; Zocchi, A.; Ward, T. R. Electrophoretic Behavior of Streptavidin Complexed to a Biotinylated Probe: A Functional Screening Assay for Biotin-Binding Proteins. *Electrophoresis* **2005**, *26*, 47−52.